

Karst spring recession and classification: efficient, automated methods for both fast and slow flow components

Tunde Olarinoye¹, Tom Gleeson², Andreas Hartmann^{1,3}

¹Chair of Hydrological Modeling and Water Resource, University of Freiburg, Germany

²Department of Civil Engineering, University of Victoria, BC, Canada

³Department of Civil Engineering, Bristol University, UK

Correspondence to: Tunde Olarinoye (tunde.olarinoye@hydmod.uni-freiburg.de)

Abstract.

Analysis of karst spring recession hydrographs is essential for determining hydraulic parameters, geometric characteristics and transfer mechanisms that describe the dynamic nature of karst aquifer systems. The extraction and separation of different fast and slow flow components constituting karst spring recession hydrograph typically involve manual and subjective procedures. This subjectivity introduces bias, while manual procedures can introduce errors to the derived parameters representing the system. To provide an alternative recession extraction procedure that is automated, fully objective and easy to apply, we modified traditional streamflow extraction methods to identify components relevant for karst spring recession analysis. Mangin's karst-specific recession analysis model was fitted to individual extracted recession segments to determine matrix and conduit recession parameters. We introduced different parameters optimisation approaches of the Mangin's model to increase degree of freedom thereby allowing for more parameters interaction. The modified recession extraction and parameters optimisation approaches were tested on 3 karst springs in different climate conditions. The results show that the modified extraction methods are capable of distinguishing different recession components and derived parameters that reasonably represent the analysed karst systems. We record an average $KGE > 0.85$ among all recession events simulated by the recession parameters derived from all combinations of recession extraction methods and parameters optimisation approaches. While there are variabilities among parameters estimated by different combinations of extraction methods, optimisation approaches and seasons, we find even much higher variability among individual recession events. We provide suggestions to reduce the uncertainty among individual recession events and raise questions on how to improve confidence in system's attributes derived from recession parameters.

1 Introduction

Groundwater from karst aquifers are essential water sources globally (Stevanović 2018; Goldscheider et al. 2020). Karst aquifers are characterized by high degree of heterogeneity and complex flow dynamics resulting from the interplay of conduit and matrix drainage systems (Király 2003; Goldscheider and Drew 2007). Groundwater flow is rapid in the highly-conductive

32 conduit system whereas it is several order of magnitude slower in the less-conductive matrix system (Goldscheider 2015).
33 While both systems have significant storage capacities, groundwater residence time is longer in the matrix than the conduit
34 system (Kovács et al. 2005).

35

36 Several methods including detailed site-specific speleological investigation (Ford and Williams 2007), tracer tests
37 (Goldscheider and Drew 2007; Goldscheider and Neukum 2010), hydrograph analysis (Kovács et al. 2005; Fiorillo 2014) and
38 model ensembles (Fandel et al. 2020) are used to characterize groundwater flow dynamics in karst systems. Aside from
39 hydrograph analysis which usually requires only spring discharge time series data, other methods are either expensive to apply,
40 time consuming or require more input. This therefore makes time series analysis a commonly applied method for karst aquifer
41 flow analyses and modelling (Ford and Williams 2007).

42

43 Quantitative time series analysis provides a lumped attributes of karst aquifer system that are rather difficult to directly measure
44 (Kovács et al. 2005). Karst spring recession analysis still remains a vital quantitative time series analysis tool for estimating
45 aquifer parameters and geometric properties (Fiorillo 2011). Discharge from karst springs reflects the complex interplay of
46 conduit and matrix systems, and provides insight about the characteristics of the aquifer which sustains the spring (Kovács et
47 al. 2005; Fiorillo 2014). This also provide essential information for flow prediction as the shape of spring hydrograph reflects
48 variable aquifer responses to different recharge pathways (Ford and Williams 2007). Since the shape of the spring hydrograph
49 describes in an integrated manner how different aquifer storages and processes control the spring flow (Jeannin and Sauter
50 1998; WMO 2008a), analyzing individual recession limbs of spring hydrograph therefore offers extensive understanding into
51 the structural, storage and behavioral dynamics of the karst system's drainage (Bonacci 1993).

52

53 Numerous studies have employed recession analyses of karst spring hydrograph to characterize karst aquifers, evaluate aquifer
54 properties, manage groundwater resources, predict low flow and estimate baseflow parameters (Padilla et al. 1994a; Dewandel
55 et al. 2003; Kovács et al. 2005; Fiorillo 2014). Derived or estimated recession coefficients are also important parameters in
56 karst models for simulating rainfall-discharge (Fleury et al. 2007; Mazzilli et al. 2019) and other process-based modelling
57 (Hartmann et al. 2013, 2014). Unlike porous media, karst systems cannot be represented by one single storage-discharge
58 function (Ford and Williams 2007). They comprise of multiple subsystems of interconnected conduit and matrix reservoirs,
59 each with their own storage-discharge characteristics (Jeannin and Sauter 1998). Recession analysis models specifically
60 developed for karst spring analysis usually comprised of two (Mangin 1975) or more (Fiorillo 2011; Xu et al. 2018)
61 independent storage-discharge transfer functions to describe drainage characteristics of different reservoirs and simulate
62 recession flows. Dewandel et al. (2003) provide general overview and main characteristics of commonly used recession models
63 and those specifically applied to karst systems.

64

65 Even though recession analysis of spring hydrographs is cheaper in terms of resources requirement to explore the flow
66 dynamics and geometry of the karst aquifer system, a major challenge in its application is the separation of the slowflow
67 (matrix-dominated) and quickflow (conduit-dominated) components. The most commonly used karst spring hydrograph
68 separation technique is the semi-logarithmic plot that usually reveals two or more segments. At least one of these segments,
69 which is typically the last, represents linear reservoir drainage and it is attributed to the slowflow (matrix) component (Bonacci
70 1993; Ford and Williams 2007). The other segment represents the quickflow (conduit) component – at times, a third segment
71 representing the mixed component is also identified. However, this approach is visually supervised and subjectively applied
72 thereby resulting in imprecise and inconsistent estimations. The amount of time required for the visual supervision exercise
73 also makes it impractical to apply this approach to large number of hydrographs or multiple recession curves, especially if
74 individual recession segment analysis is to be considered for parameters estimation.

75

76 However, in other fields of hydrology, there are a handful of automated recession extraction methods that have been developed
77 for extracting streamflow recessions (Arciniega-Esparza et al. 2017). These traditional extraction methods aimed to explicitly
78 identify baseflow recession periods by using different statistical indices to detect less variable flow conditions. During
79 baseflow, streamflow is essentially supported by groundwater storage which provides a less variable flow condition.
80 Contributions from runoff and other unregulated sources that produce high variable flow during quick flow recession are
81 discarded by these extraction routines (Vogel and Kroll 1996; Brutsaert 2008). Although, these methods were developed to
82 extract baseflow recession from stream hydrographs, yet there is possibility to adapt them for extracting matrix and conduit
83 flow recessions of karst springs. In addition to identifying the slow flow recession component, such adaptation will focus on
84 recognizing the quick flow component instead of discarding it. But as these methods are based on different statistical indices
85 for identifying the baseflow regime, they perform differently and produce differing recession parameters (Stoelzle et al. 2013;
86 Santos et al. 2019). Therefore, while attempting to modify these routines, it is also important to explore and compare the
87 differences in the estimated recession parameters that would result from adapting these commonly used traditional recession
88 extraction methods.

89

90 Following the extraction of recession events, the estimation of recession parameters is then done either by analysing the
91 individual recession segment (IRS) or constructing a master recession curve (MRC) from all events. The MRC approach is
92 commonly used in karst hydrology studies to estimate spring recession parameters, though this approach is also considered to
93 be very biased towards long recession events (Jachens et al. 2020). Also, the single parameters' value derived from this
94 approach does not represent the actual dynamic nature and implicit heterogeneity of karst systems. However, parameters
95 derived from IRS analysis better describe the range of the aquifer system dynamics as well as understanding the seasonal

96 controls on recession behaviour (WMO 2008b). While seasonal control on recession has been widely studied in porous media,
97 studies assessing seasonal effects on karst spring recession are still rare. An advantage of the modified extraction methods
98 herein presented in study is that, it allowed us to employ the IRS analysis for parameter estimation, as well as projecting the
99 analysis along seasonal dimensions.

100

101 Hence, this study aims to develop and test a robust and objective method for extracting karst spring recession components as
102 well as determining the parameters associated with the different components of karst drainage systems. Therefore, in this study
103 we develop an automated karst recession extraction methods that can identify matrix and conduit components of karst spring
104 recession hydrograph by modifying the traditional streamflow recession extraction routines. We then estimate conduit and
105 matrix recession parameters of the IRS by using the combination of different modified recession extraction methods and
106 parameters optimisation approaches of karst recession model. We explore the effect of seasonal influences on the karst conduit
107 and matrix recession parameters as well as the aquifer system classification. Finally, the performances of the different
108 combinations of modified extraction methods and karst recession model parameters optimisation approaches were evaluated.

109

110 **2 Data and Methods**

111 To develop an automatic karst-specific recession extraction and analysis procedure that is objective and applicable to large
112 hydrograph samples, we first explore the applicability of traditional recession extraction procedures originally developed for
113 non-karst streamflow recessions (Vogel and Kroll 1992; Brutsaert 2008; Aksoy and Wittenberg 2011). Then we analyse karst
114 recession parameters using a two-reservoirs parallel drainage recession model (Mangin 1975). In the following subsections,
115 we described the recession extraction and analysis model, parameters optimisation approaches, as well as the various
116 adaptations and modifications implemented. For consistency, we use the terms ‘quickflow’ for the turbulent flow from highly
117 conductive karst drainage pathways (synonymous with conduit and storm flow) and ‘slowflow’ for the laminar flow
118 contribution from less conductive fissures and pores (synonymous with matrix, diffuse and base flow) (Atkinson 1977; Larson
119 and Mylroie 2018).

120 **2.1 Adapting streamflow methods to extract matrix and conduit recession components**

121 We adapt three different streamflow recession methods (Vogel and Kroll 1992; Brutsaert 2008; Aksoy and Wittenberg 2011)
122 to extract matrix and conduit recession components (Table 1), herein called recession extraction methods (REMs). To develop
123 an automated base flow recession extraction routine, Vogel and Kroll (1992) firstly smoothed the stream hydrograph using
124 a 3-day moving average. Thereafter, the decreasing segments of the 3-day moving average are selected as the recession
125 hydrographs. Only segments with 10 or more consecutive days are recognised as recession candidates. To exclude surface and

126 storm runoff influence at the beginning of recession, the first 30% of each recession segment is deleted. Additionally, the
127 difference between two consecutive streamflow values must be $\leq 30\%$ for the pairs to be accepted. All recession segments that
128 satisfy these conditions are then accepted as **slow flow** recessions segment.

129

130 In order to objectively determine streamflow recession that is derived purely from a dry or low flow period, Brutsaert (2008)
131 introduced **a more strict** recession extraction method. For streamflow Q , during time t , the Brutsaert method eliminates data
132 point with increased or zero values of dQ/dt , as well as points with abrupt dQ/dt values. To exclude data points that might be
133 influenced by storm runoff, three data points after a positive or zero dQ/dt are removed - in major events, an additional fourth
134 data point is removed. While Brutsaert (2008) did not provide a description for a major event, **Stoelzle et al. (2013)** applied
135 the Brutsaert method in their study and defined major event as streamflow values exceeding 30% streamflow frequency.
136 Therefore, our study uses this definition of major event from Stoelzle et al. (2013). Furthermore, the Brutsaert method also
137 excludes last two data points before a positive or zero dQ/dt and spurious data points with larger $-dQ/dt$ values.

138

139 Aksoy & Wittenberg (2011) extracted the baseflow component from daily streamflow hydrograph during recession by
140 comparing the coefficient of variation (CV) of the recession segment. All days with decreasing or equal observed flowrate
141 observations are considered as part of the recession curve. **Subsequently, a non-linear reservoir model (Eq. 1) is iteratively**
142 **fitted to the recession curve until the CV is ≤ 0.1 .** The CV is defined as the ratio of standard deviation between observed
143 flowrates measurements (Q_s) and calculated flowrate (Q_{calc}) to the mean of the observed flowrates as expressed by Eq. 2.
144 Segment of the recession curve with the $CV \leq 0.1$ is selected as the real baseflow recession, otherwise excluded. Only recession
145 curves with 5-day periods or longer are considered. If the number of days becomes less than 5 during iterative curve fitting
146 and $CV \leq 0.1$ is not achieved, such recession event is discarded (Aksoy and Wittenberg 2011). **To ensure consistency between**
147 **the extraction method and Mangin recession model used in this study (see Section 2.2), the value of b in Eq. 1 is set to 1,**
148 **thereby making it a linear model.**

149

150

$$151 \quad Q_t = Q_0 \left[1 + \frac{(1-b)Q_0^{1-b}}{ab} \right]^{\frac{1}{b-1}} \quad (1)$$

152

153

$$154 \quad CV = \sqrt{\frac{n^2}{n-1} \frac{\sum(Q-Q_{calc})^2}{\sum(Q)^2}} \quad (2)$$

155

156 The three recession extraction approaches (Vogel and Kroll 1992; Brutsaert 2008; Aksoy and Wittenberg 2011) were
 157 specifically developed to extract streamflow recessions that are mainly from slow flow contribution. Thus, rules and exclusion
 158 criteria specified by each method aim at eliminating the quickflow influences from the extracted recession segments. In karst
 159 systems, concentrated rapid flow through the conduit networks constitutes the quickflow, while the contribution from slow-
 160 velocity drains through the matrix pores constitutes the slowflow. The quick and slow flow represents flows from two different
 161 drainage structures and both contribute to karst spring recession (Fiorillo, 2014; Ford & Williams, 2007; Padilla et al., 1994).
 162
 163 Adapting the streamflow methods for karst spring recession analysis requires both slow and quick flow components to model
 164 matrix and conduit spring discharges. So, to adapt the traditional REMs, we (i) extract spring flow recession curve based on
 165 the specific method approach, (ii) attribute part of the recession curve that satisfies the specified method's exclusion criteria
 166 as slowflow (matrix) component, and (iii) assign the remaining part that is excluded as quickflow (conduit) component. Table
 167 1 provides an overview of the rule-based baseflow recession extraction methods and changes made in adapting them to include
 168 quickflow component of recession.

170 **Table 1: Criteria for recession extraction methods (REMs)**

Recession extraction method	General Criteria	Filter	Slow flow selection	Adaptation for quick flow selection
Vogel	Decreasing 3-day moving day average	First 30% days	$Q_t \geq 0.7Q_{t-1}$	First 30% days, $Q_t < 0.7Q_{t-1}$
Brutsaert	$\frac{dQ}{dt} < 0$	First 3 – 4, and last 2 days	$dQ_t/dt < dQ_{(t-1)}/dt$	First 3 or 4 days, $dQ_t/dt > dQ_{(t-1)}/dt$
Aksoy	$\frac{dQ}{dt} \leq 0$	-	$CV \leq 0.10$	$CV > 0.10$

172 **2.2 Karst spring recession analysis**

173 **2.2.1 Mangin model**

174 After extraction, we apply Mangin's (1975) recession analysis model which has been widely used for estimating drainage
 175 characteristics and aquifer dynamics in fractured non-homogeneous media (Fleury et al. 2007; Liu et al. 2010; Xu et al. 2018;
 176 Schuler et al. 2020; Sivelle 2020). To analyse the extracted recessions, we use this method which considers a two-component
 177 recession curve by distinguishing between quick flow (mostly through karstic conduits) and slow flow (mostly through the
 178 fissure matrix of the carbonate rock) recessions (Figure 1). Mangin presented two equations: Eq.3 describes the linear storage-
 179 discharge relationship from the saturated zone during slowflow condition represent by the Maillet (1905) equation.

180

181 $\Phi_t = Q_{r0} e^{-\alpha t}$ (3)

182

183 where Q_{r0} is the baseflow contribution at the beginning of recession when $t = 0$, α is the recession coefficient with a unit of T^{-1}
 184 and t is the lapsed time between discharge at any time t , Q_t and initial discharge at $t = 0$, Q_0 ; and Eq. 4 describes the non-
 185 linear relationship during quickflow recession from the unsaturated zone.

186

187 $\Psi_t = q_0 \frac{1-\eta t}{1+\varepsilon t}$ (4)

188

189 where q_0 is the difference between Q_0 and Q_{r0} , parameter η describes the infiltration rate through the unsaturated zone. The
 190 parameter is defined as $1/t_i$ for the duration of quickflow recession between $t = 0$ and $t_i = 1/\eta$. ε in T^{-1} unit describes the
 191 regulating capacity of the unsaturated zone during infiltration and characterises importance of concavity of quickflow recession
 192 (Padilla et al. 1994). The algebraic sum of Eq. 3 and 4 gives Eq. 5, which defines the discharge at time t during the recession
 193 period.

194

195 $Q_t = \Phi_t + \Psi_t$ (5)

196

197 Since t_i is the point of intersection of slowflow and quickflow component of the recession curve and infiltration stopped when
 198 $t > t_i$ ($t > 1/\eta$), so the quickflow component ψ_t in Eq. 5 is essentially assumed to be zero at that point ($\psi_t = 0$) (Ford and Williams
 199 2007; Civita and Civita 2008). Therefore, the application of the Mangin's model require, firstly fitting the slowflow component
 200 ϕ_t , to the slowflow segment of recession curve using Eq. 3 to determine the recession coefficient α . Afterwards, Eq. 5 is then
 201 fitted to determine the η and ε parameters of the quickflow segment. However, the accuracies of Q_{r0} , t_i and the linear
 202 representativeness of the slowflow component of the recession curve is critical for the reliable estimation of recession
 203 coefficients (Ford and Williams 2007).

204 **2.2.2 Mangin classification framework**

205 Following the estimation of recession parameters α , η and ε using Eqs 3 – 5 above, Mangin proposed a classification scheme
 206 for karst systems based on two additional parameters: (1) aquifer regulation capacity, K , and (2) infiltration delay, i . To
 207 determine K , the dynamic volume, V_{dyn} , which is defined as the volume of water stored in the phreatic zone at the peak
 208 discharge time t_0 is calculated using Eq. 6. The average volume of water, V_{ann} , discharged through the spring's outlet over one
 209 hydrological year is also calculated. The regulation capacity K , is therefore given by the ratio of V_{dyn} and V_{ann} as expressed
 210 with Eq. 7. This parameter represents the extent of the phreatic zone and its ability to regulate groundwater release from

211 storage. While porous aquifers can have values of $K > 0.5$, a typical karst system is expected to have $K < 0.5$ (Marsaud 1997;
212 Dubois et al. 2020).

213

$$214 \quad V_{dyn} = \frac{Q_{ro}}{\alpha} \quad (6)$$

215

$$216 \quad K = \frac{V_{dyn}}{V_{ann}} \quad (7)$$

217

218 The infiltration delay, i , which represents the retardation between infiltration through the unsaturated zone and spring's outlet.

219 It is calculated as the value of the quickflow component at the second day ($t = 2$) of recession (Eq. 8). The value of i ranges

220 between 0 and 1, where a system characterized by fast infiltration would have a value close to zero and slow infiltrating system

221 tends towards 1.

$$222 \quad i = \frac{1-\eta*2}{1+\varepsilon*2} \quad (8)$$

223 With the parameters K and i , five classes of karst systems are defined (also see Fig A1): (1) Well developed system (2) Well

224 developed speleological network with large downstream flood plains (3) Upstream karstification with retarded infiltration (4)

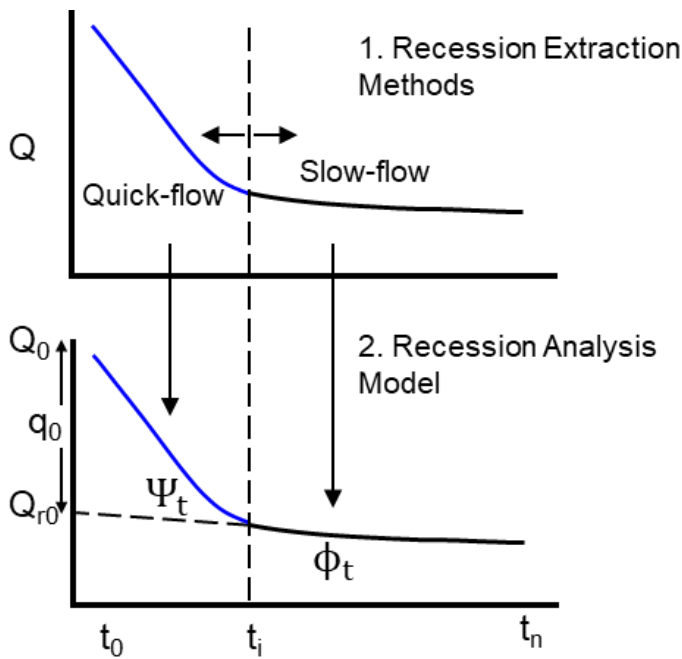
225 Complex system and (5) Poorly developed system. Ford and Williams (2007) provided a detailed review of karst aquifer

226 recession analysis and application of the Mangin model.

227

228

229



230

231 Figure 1. An illustration of karst spring recession curve showing separation into linear and non-linear components by recession
 232 extraction method and fitting appropriate components of recession analysis model.

233 2.3 Estimation of recession parameters

234 For this study, the parameters are estimated for individual, automatically extracted recession events. That way, we capture
 235 variability of spring discharge across individual recharge events (Jachens et al. 2020). To assess the effects of seasonal variation
 236 on the karst spring recession parameters, we separated the extracted events to summer and winter events. For simplicity, events
 237 that occurred between April and September of the hydrological year are considered as summer events while those from October
 238 to March are recognised as winter events. As mentioned in subsection 2.2, in the standard Mangin's approach, the slowflow
 239 component of the recession curve (Eq. 3) is fitted at first to determine α . Also, the η parameter of the quickflow component
 240 (Eq. 4) which is equivalent to $1/t_i$ is predetermined, meaning that quick flow abruptly ends at t_i days, which cannot be
 241 considered optimal. Hence, reliable determination of t_i through the extraction routines (REMs) is vital for estimation of
 242 recession parameters. These standard procedures involve with the application of Mangin's model result in less degree of
 243 freedom for parameter interaction and unrealistic abrupt ending of quick flow after t_i days. To increase the degree of freedom
 244 and assess the importance of t_i and the effect of a priori estimated η ($1/t_i$) on the Mangin's recession model, we introduced
 245 three optimization approaches which are referred to as three different parameters optimisation approaches (POAs) used in this
 246 study.

247

- 248 • **M1:** This follows the standard approach for applying the Mangin model as described by Padilla et al (1994) and Ford
 249 and Williams (2007). The slowflow component of the recession curve is fitted first with Eq. 3 for $t_i \leq t \leq t_n$ to determine
 250 α value while the quickflow component is assumed to be zero during this period. Afterwards, the second parameter

251 ε is optimised by fitting the quickflow component with Eq. 5 using the REM predefined values of η parameter (η
 252 $=1/t_i$) for the event duration between $t_0 \leq t < t_i$.

253

254 • **M2:** The conventional approach for fitting the Mangin model (M1) does not provide for independent or flexible
 255 estimation of η . The prior definition of η as $1/t_i$ rely on the accuracy of the extraction method to detect the point of
 256 inflexion t_i . This however does not give the flexibility to optimised η to a value that could provide better fit for the
 257 model. To provide for more flexible estimation of η , α parameter is determined as in M1, then Eq. 5 is fitted to the
 258 complete segment of recession curve for $t_0 \leq t \leq t_n$ to determine best values of ε and η parameters.

259

260 • **M3:** This is a very flexible approach that allows for α , ε , η and Q_{ro} values to be fitted numerically. The determination
 261 of t_i and Q_{ro} does not depend on the extraction method, rather the best fit for the parameters are obtained from
 262 optimisation process. The Mangin model (Eq. 5) is fitted to entire recession curve, which allows for absolute
 263 flexibility of t_i and robust parameters interaction during optimisation. With the model calibrated t_i ($1/\eta$), separating
 264 the quick- and slowflow segments now entirely rely on the optimisation exercise rather than extraction techniques.

265

266 For the optimisation exercise, a non-linear least squares procedure with spring discharge records was used. To avoid having
 267 negative value of conduit drainage contribution when the optimised t_i ($1/\eta$) is greater than the elapsing t value, the quick flow
 268 component, ψ_t (Eq. 4), is constrained to a minimum value of zero. Table 2 provides summary of the different optimisation
 269 approaches, parameters that were optimised as well as duration of the optimised corresponding flow component.

270

271 Table 2: Optimised recession parameters for the three different parameters optimisation approaches (POAs) of the Mangin
 272 recession analysis model.

Optim. approach	Optimized parameters	Condition	Slowflow component	Quickflow component	Degree of freedom
M1	α, ε	$\eta = 1/t_i$	$t_i \leq t \leq t_n$	$t_0 \leq t \leq t_i$	Less flexible
M2	$\alpha, \varepsilon, \eta$	$\eta \neq 1/t_i$	$t_i \leq t \leq t_n$	$t_0 \leq t \leq t_n$	Intermediate
M3	$\alpha, \varepsilon, \eta, Q_{ro}$	$\eta \neq 1/t_i$	$t_0 \leq t \leq t_n$	$t_0 \leq t \leq t_n$	Very flexible

273

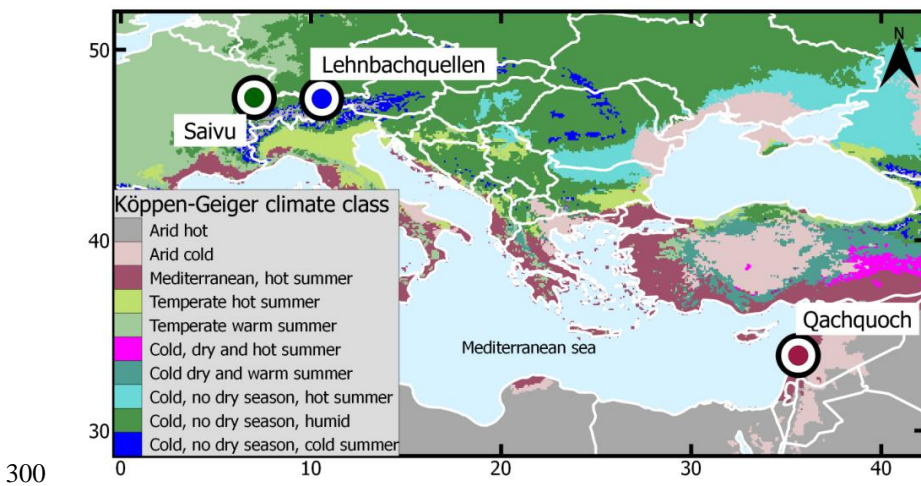
274 2.4 Comparison and evaluation of REMs and POAs

275 The three REMs (Vogel, Brutsaert and Aksoy) are combined with the three POAs (M1, M2 and M3) of the recession model
 276 to derive slow and quick flow recession parameters of selected karst springs for a total of nine possible methods. The recession

277 parameters are derived separately for both summer and winter recession events. The overall performance of the different REM
278 and POA combination is determined by calculating the goodness of fit between observed spring recession discharges and ones
279 simulated with the derived parameters using Kling Gupta Efficiency (KGE) measures (Gupta et al. 2009). We use KGE because
280 it considers the common model error types - the mean error, variability and the dynamics. The mean and interquartile ranges
281 of the derived parameters are compared among different method pairs and seasons. The estimated recession parameters were
282 used to identify the dynamic of the systems according to Mangin's karst system classification described in subsection 2.2.2.
283 The Mangin classification scheme describes the aquifer drainage characteristics, conduit development and speleological
284 network (Mangin 1975; El-Hakim and Bakalowicz 2007). Therefore, this is used to evaluate the representativeness of recession
285 parameters estimated for the selected karst springs aquifer systems.

286 **3 Test springs and data**

287 The REMs and POAs were tested using three karst springs; Lehnbachquellen, Saivu and Qachquoch located in Austria,
288 Switzerland and Lebanon respectively (Figure 2). The selection of these springs were based on geographical spread which
289 covers different climate and hydrological settings, availability of discharge hydrograph in high resolution as well as literature
290 reference on hydrological characterisation of aquifer systems drained by the spring. Daily and sub-daily spring discharge time
291 series of the selected springs were obtained from WoKaS database (Olarinoye et al. 2020). Important characteristics of the
292 spring hydrographs as well as the catchments in which they are sited are presented in (Table 3). The springs are sited in
293 catchments distinguished by different climate conditions according to the Köppen-Gieger classification (Beck et al. 2018).
294 Lehnbachquellen is sited in snow-dominated, Saivu in humid and Qachquoch is in the Mediterranean catchment. It should be
295 noted that in snow catchment, recession behaviour will be externally influenced by snow storage. However, we have included
296 snow-dominated catchment in this study to access this impact of this external influence. The spring discharge time series
297 measured at a uniform time-step for each spring span between 3 and 13 years. All discharge time series were aggregated to
298 daily temporal resolution, and missing data values which were only found (<0.01%) in Lehnbachquellen spring discharge data
299 were excluded.



300
301 Figure 2. Map showing locations of the three test springs obtained from the WoKaS database and different Köppen-Geiger
302 hydroclimatic classes.

303 Table 3. Summary of test springs site properties and characteristics of spring discharge hydrographs.

Properties	Lehnbachquellen	Saivu	Qachquoch
Climate description	Snow-dominated	Humid	Mediterranean
Spring elevation (masl)	1293	371	65
Köppen-Geiger	Cold and no dry season	Cold and humid	Mediterranean, hot summer
Temporal res.	Daily	Hourly	Sub-hourly
Length	1999-2012	1993-1995	2014-2018
Missing data	<0.01%	0	0
Mean discharge (m ³ /s)	0.06	0.29	1.08
Mean precipitation (mm/y)	1396	1201	523

304

305 4 Results

306 4.1 Extracted recessions and performance of POAs

307 The adapted recession extraction methods adequately identified karst spring conduit and matrix flow components. The
308 parameters obtained with the different REM-POA pairs also produced a satisfactory simulations of recession events. Only
309 complete recession events ≥ 7 days period were considered for analysis. Here, complete recession referred to events that
310 featured both conduit and matrix components. For each spring hydrograph, a different number of recession events are identified
311 by the REMs. As shown on Table 4, Vogel method captured the highest number of recession events across all springs, followed
312 by Brutsaert (except for Lehnbachquellen spring) and Aksoy showed the least ability to capture recession periods from the
313 observed spring discharges. However, the average length of the recession events varied among the different REMs in no

314 particular order (see Fig. A2 in appendices). Based on the number of recognizable recession events, the REMs were defined
 315 as permissive (Vogel), less permissive (Brutsaert) and restrictive (Aksoy).

316

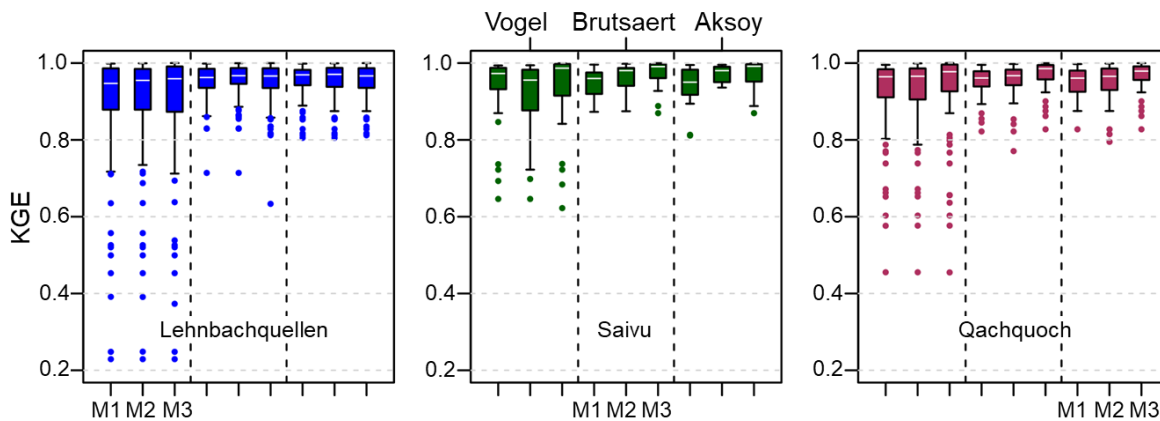
317 Table 4: Recession events period extracted by the REMs for the three spring discharge hydrographs

REM	Lehnbachquellen			Saivu			Qachquoch		
	Total	Summer (%)	Winter (%)	Total	Summer (%)	Winter (%)	Total	Summer (%)	Winter (%)
Vogel	157	0.53	0.47	33	0.42	0.58	41	0.37	0.63
Brutseart	122	0.39	0.61	25	0.48	0.52	36	0.47	0.53
Aksoy	146	0.50	0.50	19	0.58	0.42	31	0.48	0.52

318

319 Figure 3 shows how the parameters derived from the different REMs and POAs combinations performed in simulating
 320 recession events using the KGE measures. With exclusion of the outliers, a high KGE value were achieved across all
 321 combinations, ranging between 0.70 and 1.0. More than half of all simulated events across the three springs produce a KGE
 322 >0.9 for all REM-POA pairs. However, the lowest performance in all three springs is related to POAs combined with Vogel
 323 extraction method. While there was no vivid observable pattern among the extraction methods (REMs) and recession model
 324 performance, the parameters optimisation approaches (POAs) showed otherwise. A clear systematic order for the KGE median
 325 is found within the POAs: M1 < M2 < M3. This is more noticeable in the humid and Mediterranean springs, except for the
 326 Vogel-M2 combination in the humid spring that is not in the systematic order.

327



328

329 Figure 3: Boxplot of KGE measures between observed and simulated recession events based on parameters derived from the
 330 different REMs and POAs. The boxplots represent the interquartile ranges of KGE with the median shown in white lines and
 331 outliers marked in coloured points.

332 4.2 Variability of recession parameters among the different REMs-POAs and seasons

333 Figure 4 Figure 5 respectively shows the results of the optimised slowflow and quickflow recession parameters for both
 334 summer and winter periods. These parameter sets are combinations of α , η and ε that produces the best simulation fit (i.e.

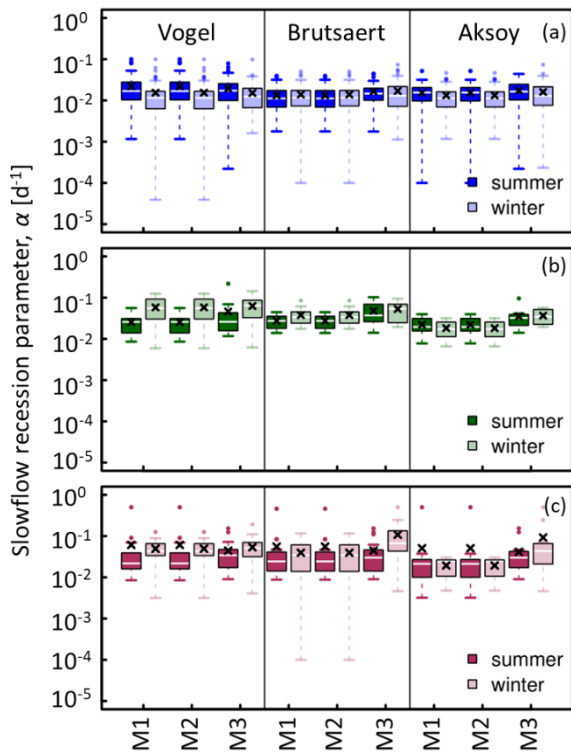
335 highest KGE value) with the different REM-POA pairs. Recession curve fitting based on the individual segment led to a large
336 number of parameter combinations with the nine possible REM-POA pairs. The modification of REMs and POAs produces
337 complex parameter interactions, for simplification, we explore the results along two dimensions: (1) variability among the
338 methods and (2) variability within seasons.

339

340 The results from Figure 4 show that REMs and POAs only have marginal effects on the estimation of recession coefficient, α ,
341 when compared to the seasonality effect. Also, there are differences on how the REMs and POAs impact the estimated values
342 of α among the three karst spring catchments. Although, the values of the mean, median and interquartile ranges of α estimated
343 by all the REMs for the snow-dominated catchment seems to be similar, but slight differences can still be observed. The
344 slowflow recession parameters estimated by the permissive REM (Vogel) are within a slightly higher ranges. On the other
345 hand, the estimation of α in the humid and Mediterranean catchments seems to be more impacted by the POAs. By increasing
346 the degree of freedom of the POAs, higher values of α are estimated, most noticeably with the M3 parameter optimization
347 approach.

348

349 While the impacts of methodological approaches (i.e., REMs and POAs) are marginal on the estimated values of α , seasonal
350 impacts on the values and variabilities of the parameter are more evident. The Saivu and Qachquoch springs in humid and
351 Mediterranean catchments respectively shows similar dynamics in terms of seasonal variability of α , while Lehnbacquellen
352 spring located in snow-dominated catchment shows a different seasonal dynamic. For Lehnbacquellen spring, the values of
353 the estimated α parameter are higher for summer recession events, noticeably with Vogel and Aksoy extraction techniques
354 (Figure 4). During summer period, estimated α values also show less variability with Vogel and Brutsaert REMs, while Aksoy
355 give a more varied results for the same season. Meanwhile, an opposite situation is seen with the Saivu and Qachquoch springs.
356 The median values and interquartile ranges of α are higher in winter for estimations done with Vogel and Brutsaert extraction
357 methods. For these springs, estimations associated with Aksoy extraction method occasionally give slightly lower α values
358 during winter and less parameter variability. For all the spring systems, the seasonal variability of α is more observable with
359 analysis associated with Vogel, which is the most permissive REM.



360

361 Figure 4. Distribution and variability of slowflow recession parameter, α , obtained by the combination of REM (Vogel,
 362 Brutsaert and Aksoy) and POA (M1, M2 and M3) for summer and winter periods: (a) Lehnbacquellen spring in snow-
 363 dominated catchment, (b) Saivu spring located in humid catchment and (c) Qachquoch spring in the Mediterranean catchment.
 364 The boxplots represent the interquartile range, whisker lines correspond to the most extreme parameter values and outliers
 365 marked as circle with corresponding box colour.

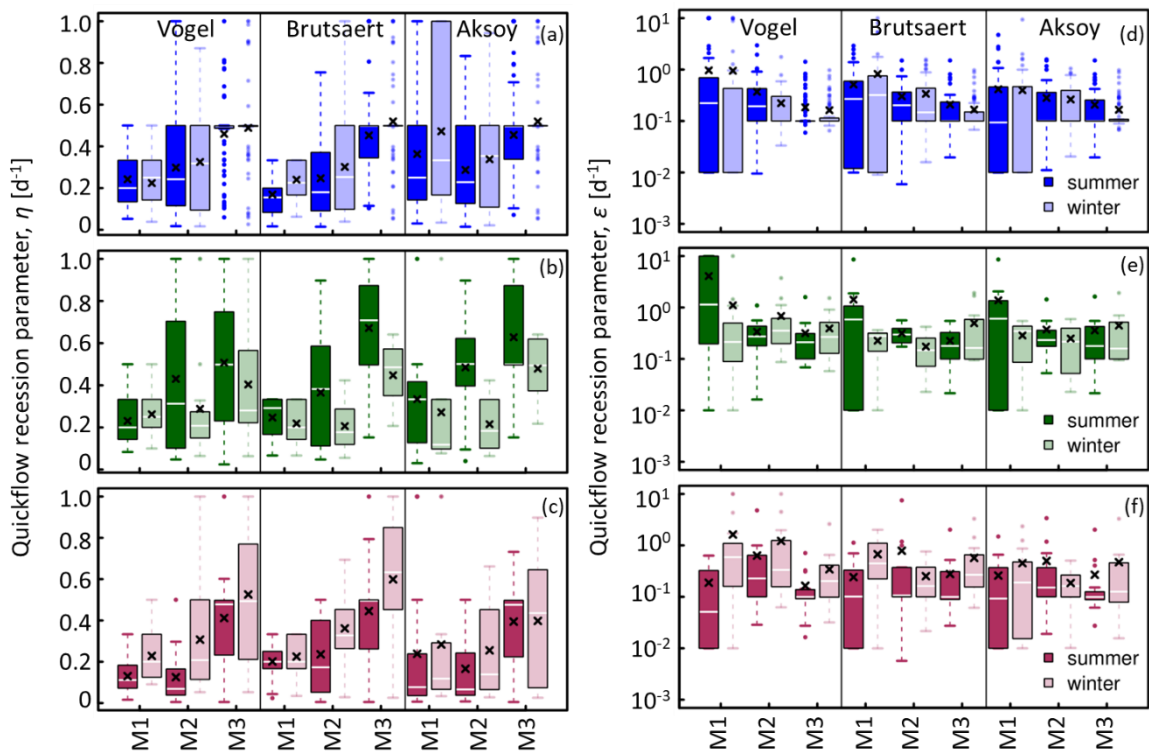
366

367 Both the recession analysis methodology (REMs and POAs) as well as seasons have significant impacts on the estimated
 368 values of infiltration rate, η , and curve concavity, ε , parameters. The most visible pattern from Figure 5 is that the increasing
 369 degree of freedom during optimisation usually results to higher estimates ($M3 > M2 > M1$) and larger variability of η . However,
 370 this pattern may slightly varies among the different spring systems. The values of η parameter span one order of magnitude
 371 for REMs and POAs combinations across all spring locations. The springs in snow-dominated (Lehnbachquellen) and
 372 mediterranean (Qachquoch) catchments show similar dynamic in terms of seasonal variation of η . The estimated median and
 373 mean values of η are higher in winter for both springs. While parameter variability between seasons is relatively comparable
 374 in the snow-dominated catchment, larger variability is seen during winter in the mediterranean catchment. In the humid
 375 catchment, the spring (Saivu) shows an opposite seasonal pattern, summer events have higher η values as well as larger
 376 variability.

377

378 Estimation of curve concavity parameter, ε , also reflects the influence of recession analysis methods and seasonal variations.
 379 The values of ε extend over three order of magnitude across the three spring locations. In a differing pattern from η , increasing
 380 the flexibility of the parametrisation approach (POA) leads to low and more consistent ε values. We observe a decreasing order
 381 of $M1 < M2 < M3$ in the estimated values of ε parameter for both summer and winter period. Although, combinations of

382 Brutsaert and Aksoy REMs with most flexible POA (M3) slightly contradict this order at times, particularly for the humid and
 383 mediterranean springs. Although the mean and median values show a slightly higher winter parameter estimations, however,
 384 the parameter ranges are similar for both summer and winter periods in the snow-dominated catchment. There is no consistent
 385 seasonal pattern in the dynamics of ε estimated for the humid and mediterranean springs. But an understated pattern seen is
 386 higher (Saivu spring - humid) or lower (Qachquoch spring – mediterranean) estimations of ε in summer, especially with M1
 387 parameterisation approach.
 388 In general, for the respective seasons, there is relatively better consistency among REM-POA pairs in estimating both slow
 389 and quick flow recession parameters as shown by the results in Figure 4 and Figure 5. In fact, there is much higher parameters
 390 variability among recession events than the different REM-POA combinations and seasons.



391
 392 Figure 5. Distribution and variability of the quickflow recession parameters, η and ε , (y-axis of ε in log scale) obtained by the
 393 combination of REM (Vogel, Brutsaert and Aksoy) and POA (M1, M2 and M3) for summer and winter periods: (a and d)
 394 Lehnbacquellen spring in snow-dominated catchment, (b and e) Saivu spring located in humid catchment and (c and f)
 395 Qachquoch spring in the Mediterranean catchment. The boxplots represent the interquartile range, whisker lines correspond to
 396 the most extreme parameter values and outliers marked as circle with corresponding box colour.

397 4.3 Aquifer characterization

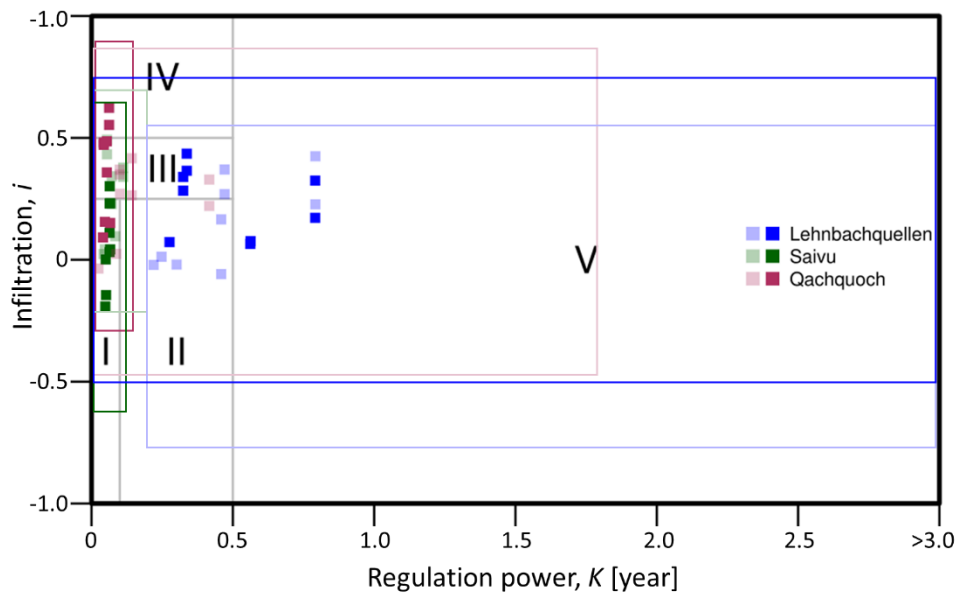
398 To evaluate the overall representativeness of estimated recession parameters based on the modified REMs and different POAs
 399 for the selected karst spring systems, we determine the drainage properties of the spring's aquifer using the parameters derived
 400 from the individual recession event. As described in subsection 2.2.2, retardation between infiltration and output defined by

401 infiltration delay parameter, i , and aquifer regulation power, K , were calculated for individual recession event. Figure 6 shows
402 the mean aquifer classifications as well as their standard deviations based on per event estimated K and i values. The values of
403 K and i are calculated for individual recession event with the recession parameters derived from the nine REM-POA
404 combinations. As shown by the standard deviation bounds of the drainage properties derived from individual recession
405 segments in Figure 6, there is an overlapping of calculated drainage properties and aquifer classes between the seasons. The
406 methodological differences in the selected REM and POA result in large variations in the calculated mean values of infiltration
407 delay, i , among the springs. The estimated mean values i for the three spring systems used in this study cover similar ranges
408 (0.20 to 0.65). With the exemption of Lehnbachquellen spring, there is a good coherency in the mean K values determined from
409 all combinations of REM and POA for each spring. In addition, the systems are more distinguishable by their ability to store
410 and regulate groundwater outflow through the springs

411
412 Among the three karst springs, only the Qachquoch spring showed a clear impact of seasonality in the system's classification.
413 In summer, the estimated mean K values are <0.1 year which is unanimous between the REM-POA combinations. Whereas
414 mean K values up to 0.45 and standard deviations of 1.75 years are estimated for the winter recessions. This results in a system
415 classification extending from of class I (well-developed system) and class IV (complex system) in summer; and a system
416 characterize as predominately class III (fairly karstified system) in winter. Groundwater has very short residence time in the
417 Saivu spring system for both summer and winter periods. The mean regulation capacity of the system is <0.1 years, although
418 a slightly higher value (ca. 0.15 years) is derived during the winter season. Due to this low regulation power, K , of the Saivu
419 spring system, it is characterized predominately as class I in both summer and winter period. Only a handful of method
420 combinations place the system in class III.

421
422 While the other two springs (Qachquoch and Saivu) show either clear or slight seasonal influence in the karst systems
423 characterization, Lehnbachquellen spring do not show a systematic seasonal impact in its characterisation. Both the estimated
424 mean infiltration delay i , and regulation power K , shows high inconsistent pattern for Lehnbachquellen spring. The mean K
425 values rang between 0.25 and 0.80 years with standard deviation values >3 years for both summer and winter recessions events.
426 With these high K values, the Lehnbachquellen system has the highest capacity to withhold groundwater among the three karst
427 springs used in this study. The wide dispersion of both K and i makes it impossible to confine the system's into a specific class.
428 The Lehnbachquellen system therefore falls within three classes; class II (well-developed system with large downstream flood
429 plains), class III and class V (poorly developed system).

430



431

432 **Figure 6. Karst aquifer type classification based on mean values of K and i calculated with recession parameters estimated by**
 433 **the different combinations of REM and POA for both summer (full-shaded colour) and winter (light-shaded colour) periods.**
 434 **Distributions of the per event mean K and i derived from all method combinations for each spring are represented by**
 435 **coloured points; areas covered by unfilled boxes are the standard deviations.**

436

437 5 Discussion

438 5.1 Quality of extracted recessions

439 With the modification of the traditional REMs, we were able to establish a completely objective approach to distinguish
 440 between slow and quick flow recession components. Furthermore, optimisation approaches (POAs) with more flexibility
 441 showed better improvement over the conventional parametrisation procedure. The REMs tested use different statistical indices
 442 to scrutinise genuine baseflow records, hence they have different level of tolerance. The ability of the extraction methods to
 443 identify recession periods from hydrograph time series depend on the level of their restrictiveness. Vogel extraction method
 444 defined by a 3-day moving average to smoothen the hydrograph and also allows for 30% increase in subsequent flowrates is
 445 more permissive than Brutsaert and Aksoy methods that strictly enforce $dQ/dt < 0$. Hence, more recession events were
 446 extracted by Vogel method. Study by Stoelzle et al. (2013) also showed the Vogel procedure to be more permissive, as it was
 447 able to extract almost 50% more events than Brutsaert. Although main recession selection condition for Brutsaert and Aksoy
 448 method is determined by decreasing dQ/dt , constraining real baseflow recessions to discharge data points with less than 10%
 449 ($CV \leq 0.1$) deviations makes the Aksoy more restrictive than Brutsaert method.

450

451 Generally, all combinations of REM-POA performed acceptably well, increasing restrictiveness of extraction method gave
452 improved model performance. Even though restrictiveness led to better performance, this should not be a basis to out-rightly
453 accept restrictive REM over less-restrictive one. For instance, standard removal of 3 or 4 days by Brutsaert method as
454 stormflow-influenced period is speculative and could led to unrealistic estimation of conduit flow duration, t_i , ($t_i = 1/\eta$), yet it
455 performed better than permissive Vogel method. Although, such problem of unrealistic t_i estimation inherent from Brutsaert
456 was eliminated and general improvement in models performances were achieved by increasing parameters flexibility during
457 optimisation. Overall, the adapted REMs and the introduced three POAs provided range of results that adequately represented
458 the karst systems. However, there are still aspects of automated recession extraction that could benefit from further
459 improvement for their general application in karst hydrology. For instance, the heterogeneous nature of karst system results in
460 very dynamic spring discharge dynamic, by introducing more tolerance to the REMs to accommodate usual karst spring
461 discharge anomaly, longer recession events could be extracted. In addition, while all REM-POA pairs are good from the model
462 performance perspective, it will be misleading to define best pair of REM-POA base on this, without first evaluating if the
463 estimated parameters are realistic.

464 5.2 Effects of recession analysis methods and seasonality on extracted recession parameters

465 5.2.1 Effects of REM-POA combinations on extracted recession parameters

466 Methodological choices of REMs and POAs combinations have impacts on the estimated recession parameters. The extent to
467 which the parameters are influenced by the methods largely varies between the slowflow and quickflow recession parameters.
468 There was relatively higher consistency and better stability among all REM-POA pairs in estimating slow flow recession
469 parameter that describe the drainage characteristics of the matrix block within the phreatic zone. Depending on the catchment's
470 hydroclimatic settings, both REM s and POAs shown to have marginal impacts on the estimation of slowflow recession
471 parameter. Though, this is slightly contrary to other studies who found that slowflow recession coefficients are majorly
472 influenced by the extraction method used, while the parameterization approach only have a marginally impact (e.g. Stoelzle et
473 al. 2013; Santos et al. 2019).

474 Although the combination of REM and POA affects the estimation of conduit drainage characteristics, the effect of the POA
475 tends to be more pronounced. Increasing degree of parameter freedom during optimisation with the different POAs
476 formulations often resulted to significant reduction in parameters variability. This was also accompanied by either low- or
477 high-estimation of conduit drainage parameters. The more flexible parameterisation approaches (M2 and M3) generally led to
478 higher infiltration rates through the unsaturated zone. Infiltration rate is predetermined ($\eta = 1/t_i$) in the original parameterisation
479 procedure of Mangin's model (M1), therefore restricted the fitting the quickflow recession curve only to the optimisation of
480 parameter ε , which regulates infiltration through the unsaturated zone. The values of ε smaller than 0.01 have been reported to
481 indicate very slow infiltration and values between 1 and 10 show a domination of fast infiltration (Ford and Williams, 2007;

482 El-Hakim and Bakalowicz, 2007). To compensate the inflexibility due to predetermined infiltration rate, the regulation effect
483 of the unsaturated zone was amplified, which was evident in the higher and more varied values of ε estimated with M1
484 parameterisation procedure. By means of excluding a fixed number of days (3-4) as influenced stage of recession, Brutsaert
485 paired with M1 also led to similar values of η estimated for all springs. This makes it an unsuitable combination, especially
486 with long recession period. In their study, Santos et al. (2019) found analysis with Brutsaert method to be more robust and
487 appropriate for short recession samples.

488 Despite the impacts of methodological choices on the uncertainty of estimated recession parameters, variability among events
489 exceeded the variability among methods. These high variabilities are attributed to different lengths of extracted recession
490 events, differences in karstic processes such as recharge, infiltration as well as conduit pathways that are activated within the
491 unsaturated and saturated zones for each event. Even though karst systems are very heterogeneous and it is important to capture
492 the impacts of the variable karstic processes through the analysis of individual recession segment, the high uncertainty among
493 events make it difficult to define a set of representative recession parameters.

494 Per event recession analysis is very useful to better understand the karst system dynamic compared to master recession analysis
495 which is unable to depict the hydrodynamic behaviour of karst. However, the high uncertainty found with this approach is still
496 a challenge and a bit difficult to cope with. We believe there are still possibility for improvement with this approach, for
497 example defining a systematic approach to quantify parameters uncertainties will help to increase the confidence of the
498 individual recession segment analysis.

499

500 **5.2.2 Seasonal influences on recession parameters**

501 The seasonal variability of slowflow recession parameter is inter-connected with the choice of REM. Among the three different
502 REMs used in this study, a clear seasonal variability of α was more noticeable with Vogel, which is the most permissive REM.
503 However, the observed seasonal variability diminished with increasing restrictiveness of the REM. Also, the pattern of the
504 seasonal variability of α was not the same for all three catchments and this emphasized the influence of climatic controls on
505 karst aquifer drainage. For instance, humid and dry regions are usually characterized by long recession and perhaps significant
506 drop in groundwater table during summer. From the results presented in previous section, we identified lower values of α in
507 summer compared to winter. As the parameter α signifies the slope of slowflow recession, a higher value means steeper slope
508 and faster emptying of the aquifer. The lower α values seen during summer emphasized the drought resistance of the system
509 due decreased in the aquifers hydraulic head. Meanwhile the snow-dominated catchment showed an opposite behaviour with
510 higher values of α in summer. This occurred due the accumulation and melting of snow. The snow melting process during the
511 summer period would result in higher hydraulic head while frozen ice packs in winter translate to lesser hydraulic gradient.

512 As previous mentioned, higher hydraulic head would promote faster drainage of the aquifer resulting in higher values of α
513 parameter.

514

515 For quickflow recession parameters, seasonal variability is independent of the REM. The three springs showed different
516 seasonal patterns which could be directly linked to their hydroclimatic settings. Seasonal influence on quickflow recession
517 parameters was not clearly seen in the snow-dominated catchment. This could be attributed to the snow melting process
518 discussed above. Since snow melt compensates hydrologic flow during warmer period, there would be constant influx from the
519 surface throughout the year, also soil wetness conditions do not change significantly. This explains the lack of any evident
520 seasonal differences between parameters η and ε estimated for in Lehnbachquellen spring in the snow-dominated catchment.
521 But the Saivu spring in the humid and Qachquoch spring in the mediterranean catchment showed clear seasonal influences.
522 Estimated values of infiltration rates η for Saivu were higher in summer (lower in winter) and lower in summer (higher in
523 winter) for the Qachquoch spring. This pattern is believed to be controlled by the peculiarity of the different geographic and
524 climatic settings. In humid catchment, higher temperature in summer would result in dryer soil conditions which would
525 consequently facilitate faster infiltration. However, for the mediterranean settings, soil conditions are dry due to relatively
526 warmer temperature all year round. This makes precipitation is a limiting factor, and with more precipitation in winter, faster
527 infiltration through the unsaturated zone would occur.

528

529 5.3 How realistic are adapted REM-POA for karst system analysis?

530 Karst system classification proposed by Mangin (1975) is based on two parameters K and i (see subsection 2.2.2). These two
531 parameters were derived from the estimated recession parameters (α , η and ε), thus the variability found in the recession
532 parameters is expected to be propagated to K and i . Although, if the derived mean values of K were considered, some level of
533 coherency was found among all REM-POA combinations and between the seasons. But looking at the estimated standard
534 deviations, a large intra-event and seasonal variation can be found. In a study by Grasso & Jeannin (1994), the authors found
535 regulation power, K , to be more stable for various years and events. These findings did not agree with our analysis, the
536 outcomes of which showed a large variability among K for different events, most significantly in the snow-dominated
537 catchment. Regulation power is analogous to memory effect, and the periodic water release from an external snow storage that
538 is not captured within the saturated zone in real time makes K to fluctuate more in snow-dominated catchment. Considering
539 the standard deviations from the mean, in fact the values of K exceeded the maximum value of 1 originally proposed in Mangin
540 karst classification scheme. Mangin (1975) set a maximum value of one for K , with assumptions that real karst systems would
541 not have a storage memory beyond one year. However, karst system in a snow catchment could have K values greater than
542 one due to snow accumulation and melting as found in Lehnbachquellen spring. Also, complex aquifer systems, as in the case
543 of Qachquoch spring could also have higher K values.

544

545 Infiltration delay, i , is strongly dependent on recharge type contribution as well as catchment size (Jeannin and Sauter 1998).

546 Recharge is control by climatic input (rainfall) which varies between seasons. However, the derived values of i were hardly

547 separated by season, but more varied among individual recession events. The complex interplay of REM and POA resulted in

548 a compensation phenomenon; whereby infiltration rate, η , was compensated by recession concavity parameter, ε . Since the

549 infiltration delay is defined by these parameters, it is difficult to explicitly infer the specific effects of REM and POA on

550 infiltration delay.

551

552 The northern Alps karst system where the Lehnbachquellen spring is located has been defined as well karstified highly

553 permeable unit interlayered with less permeable Flysch formation (Goldscheider 2005; Chen et al. 2018). Our analysis partly

554 placed the karst system in class II and III thereby showing some consistency with literature evidence. Perrin, Jeannin, &

555 Zwahlen (2003) described Saivu spring system as a well-developed karstic network, majority of the methods pair used in this

556 study place this spring in class 1, therefore coherently agreeing with the authors description. Taking in account the standard

557 deviations, the classification of Qachquoch spring ranged between medium to poorly karstified system. This is similar to a

558 recent study by Dubois et al. (2020) that categorises the system as poorly karstified with a very large regulation capacity.

559

560 Given that existing common karst spring recession extraction method involves visually supervised procedure and subjectively

561 determined duration of conduit infiltration, alternative faster, automated and objective approach is very useful. From our

562 analysis, resulting parameters of extracted recession segments are within reasonable ranges and derived systems classification

563 correspond to those found in literatures. The good performance recorded between simulated and observed flowrates during

564 recession events attests to the potential transferability of traditional extraction methods to karst systems. However, this good

565 performance does not necessarily translate to reliable parameter estimates. It is therefore important to choose REM methods

566 that gives reasonable parameters especially when paired with a less flexible optimisation approach. Furthermore, with prior

567 knowledge of the spring system, parameters ranges can be reasonably constrained during optimisation to achieve more

568 representative optimum parameters.

569

570 **6 Conclusions**

571 The application of karst spring hydrographs recession analysis is very broad, including estimation of storage capacity (Fleury

572 et al. 2007), describing discharge of unsaturated zone (Amit et al. 2002; Mudarra and Andreo 2011) as well as systems

573 classification (El-Hakim and Bakalowicz 2007). Most often manual recession extraction is used and the high subjectivity of

574 the approach introduces bias to estimated parameters. For the first time in literatures, this study explores the applicability of

575 automated traditional recession extraction methods (REMs) originally developed for slow flow (baseflow) recession by
576 adapting them to also identify quick flow flow recessions. We fit individual extracted recession segments with Mangin's
577 recession model to determine the conduit and matrix drainages recession characteristics. We introduce new parameters
578 optimisation approaches (POAs) different from the conventional procedure to increase degree of freedom of parameter
579 interaction.

580

581 While we found that there were uncertainties in the estimated recession parameters resulting from the methodological choices
582 (REM and POA combinations) and seasonal influences, the uncertainties among individual recession events were much larger.
583 The large variability among individual event actually reflected the dynamic and heterogenous nature of the karst system. The
584 combination of this with REMs, POAs and seasons resulted in a more complex interplay and only amplified the uncertainties.
585 These uncertainties is actually useful to understand the dynamic nature karst system, but it is difficult to cope with and also
586 need to be systematically quantified. To avoid these large uncertainties, master recession analysis approach has being a popular
587 alternative for karst spring hydrograph analysis. But a single recession parameters' values derive from the master recession
588 approach does not reflect the highly dynamic nature of karst system. The uncertainty of karst recession parameters derived
589 from either single or master recession approach is presently not a discussion in karst hydrology. Maybe such discussion needs
590 to start to address the limitations and difficulties encountered in this study. Herein, we pose two major issues that need to be
591 addressed as seen from this study: (1) how can we do recession analysis more objectively with a single REM and separation
592 technique that accounts for all ranges and possible instances of slow and quick flow? and (2) how can we incorporate a more
593 robust parameters estimation and uncertainty quantification approach into individual recession analysis? Answering these
594 questions will help to expand confidence in the system's drainage characteristics that are derived from recession parameters.

595

596 Finally, this study has shown that there are a lot of potentials for extracting and separating karst spring recession components
597 by adapting the traditional REMs and introducing flexible parameter optimization approaches. The adaptation of the REMs in
598 combination with the different parameters estimation flexibility (POAs) provides a suit of automated tools that can be used for
599 karst recession study. This automated and multi approach for parameters optimization is essential to cope with the known
600 biases of single and visually supervised recession analysis methods. Different REMs has their specific advantages and there
601 are still room for improvement. For example, other extraction can could be tested and non-linear reservoir model can also be
602 considered for fitting the matrix model.

603

604 *Acknowledgements.*Support to T.O. and A.H was provided by the Emmy Noether Programme of the German Research
605 Foundation (DFG; grant no. HA 8113/1-1; project "Global Assessment of Water Stress in Karst Regions in a Changing
606 World").

607

608 **Code availability**

609 The R codes for the different REMs and POAs used for the recession analysis can be accessed through our GitHub repository
610 here <https://github.com/KarstHub/Karst-recession>

611 **References**

612 Aksoy H, Wittenberg H (2011) Nonlinear baseflow recession analysis in watersheds with intermittent streamflow. *Hydrol Sci*
613 *J* 56:226–237. <https://doi.org/10.1080/02626667.2011.553614>

614 Amit H, Lyakhovsky V, Katz A, et al (2002) Interpretation of Spring Recession Curves. *Ground Water* 40:543–551.
615 <https://doi.org/10.1111/j.1745-6584.2002.tb02539.x>

616 Arciniega-Esparza S, Breña-Naranjo JA, Pedrozo-Acuña A, Appendini CM (2017) HYDRORECESSION: A Matlab toolbox
617 for streamflow recession analysis. *Comput Geosci* 98:87–92. <https://doi.org/10.1016/j.cageo.2016.10.005>

618 Atkinson T. (1977) DIFFUSE FLOW AND CONDUIT FLOW IN LIMESTONE TERRAIN IN THE MENDIP HILLS,
619 SOMERSET (GREAT BRITAIN). *J Hydrol* 35:93–110

620 Beck HE, Zimmermann NE, Mcvicar TR, et al (2018) Data Descriptor: Present and future Köppen-Geiger climate
621 classification maps at 1-km resolution. <https://doi.org/10.1038/sdata.2018.214>

622 Bonacci O (1993) Karst springs hydrographs as indicators of karst aquifers. *Hydrol Sci J* 38:51–62.
623 <https://doi.org/10.1080/02626669309492639>

624 Brutsaert W (2008) Long-term groundwater storage trends estimated from streamflow records: Climatic perspective. *Water*
625 *Resour Res* 44:. <https://doi.org/10.1029/2007WR006518>

626 Chen Z, Hartmann A, Wagener T, Goldscheider N (2018) Dynamics of water fluxes and storages in an Alpine karst catchment
627 under current and potential future climate conditions. *Hydrol Earth Syst Sci* 22:3807–3823. [https://doi.org/10.5194/hess-](https://doi.org/10.5194/hess-22-3807-2018)
628 [22-3807-2018](https://doi.org/10.5194/hess-22-3807-2018)

629 Civita M V, Civita M V (2008) An improved method for delineating source protection zones for karst springs based on analysis
630 of recession curve data. *Hydrogeol J* 16:855–869. <https://doi.org/10.1007/s10040-008-0283-4>

631 Dewandel B, Lachassagne P, Bakalowicz M, et al (2003) Evaluation of aquifer thickness by analysing recession hydrographs.
632 Application to the Oman ophiolite hard-rock aquifer. *J Hydrol* 274:248–269. [https://doi.org/10.1016/S0022-](https://doi.org/10.1016/S0022-1694(02)00418-3)
633 [1694\(02\)00418-3](https://doi.org/10.1016/S0022-1694(02)00418-3)

634 Dubois E, Doummar J, Pistre S, Larocque M (2020) Calibration of a lumped karst system model and application to the
635 Qachqouch karst spring (Lebanon) under climate change conditions. *Hydrol Earth Syst Sci* 24:4275–4290.
636 <https://doi.org/10.5194/hess-24-4275-2020>

637 El-Hakim M, Bakalowicz M (2007) Significance and origin of very large regulating power of some karst aquifers in the Middle

638 East. Implication on karst aquifer classification. *J Hydrol* 333:329–339. <https://doi.org/10.1016/j.jhydrol.2006.09.003>

639 Fandel C, Ferré T, Chen Z, et al (2020) A model ensemble generator to explore structural uncertainty in karst systems with
640 unmapped conduits. *Hydrogeol J*. <https://doi.org/10.1007/s10040-020-02227-6>

641 Fiorillo F (2014) The Recession of Spring Hydrographs, Focused on Karst Aquifers. *Water Resour Manag* 28:1781–1805.
642 <https://doi.org/10.1007/s11269-014-0597-z>

643 Fiorillo F (2011) Tank-reservoir drainage as a simulation of the recession limb of karst spring hydrographs. *Hydrogeol J*
644 19:1009–1019. <https://doi.org/10.1007/s10040-011-0737-y>

645 Fleury P, Plagnes V, Bakalowicz M (2007) Modelling of the functioning of karst aquifers with a reservoir model: Application
646 to Fontaine de Vaucluse (South of France). *J Hydrol* 345:38–49. <https://doi.org/10.1016/j.jhydrol.2007.07.014>

647 Ford D, Williams P (2007) *Karst Hydrogeology and Geomorphology*. John Wiley and Sons, Ltd

648 Goldscheider N (2015) Overview of Methods Applied in Karst Hydrogeology. In: Stevanović Z (ed) *Karst Aquifers---*
649 *Characterization and Engineering*. Springer International Publishing, Cham, pp 127–145

650 Goldscheider N (2005) Fold structure and underground drainage pattern in the alpine karst system Hochifen-Gottesacker.
651 *Eclogae Geol Helv* 98:1–17. <https://doi.org/10.1007/s00015-005-1143-z>

652 Goldscheider N, Chen Z, Auler AS, et al (2020) Global distribution of carbonate rocks and karst water resources

653 Goldscheider N, Drew D (2007) *Methods in Karst Hydrogeology*. International Contributions to Hydrogeology 26,
654 International Association of Hydrogeology. Taylor & Francis, London

655 Goldscheider N, Neukum C (2010) Fold and fault control on the drainage pattern of a double-karst-aquifer system,
656 winterstaude austrian alps. *Acta Carsologica* 39:173–186. <https://doi.org/10.3986/ac.v39i2.91>

657 Gregor M, Malík P (2012) Construction of master recession curve using genetic algorithms. *J Hydrol Hydromechanics* 60:3–
658 15. <https://doi.org/10.2478/v10098-012-0001-8>

659 Gupta H V., Kling H, Yilmaz KK, Martinez GF (2009) Decomposition of the mean squared error and NSE performance
660 criteria: Implications for improving hydrological modelling. *J Hydrol* 377:80–91.
661 <https://doi.org/10.1016/j.jhydrol.2009.08.003>

662 Hartmann A, Mudarra M, Andreo B, et al (2014) Modeling spatiotemporal impacts of hydroclimatic extremes on groundwater
663 recharge at a Mediterranean karst aquifer. *Water Resour Res* 1–15. <https://doi.org/10.1002/2014WR015685>

664 Hartmann A, Weiler M, Wagener T, et al (2013) Process-based karst modelling to relate hydrodynamic and hydrochemical
665 characteristics to system properties. *Hydrol Earth Syst Sci* 17:3505–3521. <https://doi.org/10.5194/hess-17-3305-2013>

666 Jachens ER, Rupp DE, Roques C, Selker JS (2020) Recession analysis revisited: impacts of climate on parameter estimation.
667 *Hydrol Earth Syst Sci* 24:1159–1170. <https://doi.org/10.5194/hess-24-1159-2020>

668 Jeannin P-Y, Sauter M (1998) Analysis of karst hydrodynamic behaviour using global approaches: a review

669 Kiraly L (2003) Karstification and Groundwater Flow. *Speleogenes Evol karst aquifers* 1:155–192

670 Kovacs A (2021) Quantitative classification of carbonate aquifers based on hydrodynamic behaviour.
671 <https://doi.org/10.1007/s10040-020-02285-w>

672 Kovács A, Perrochet P, Király L, Jeannin PY (2005) A quantitative method for the characterisation of karst aquifers based on
673 spring hydrograph analysis. *J Hydrol* 303:152–164. <https://doi.org/10.1016/j.jhydrol.2004.08.023>

674 Kresic N, Bonacci O (2010) Spring discharge hydrograph

675 Larson EB, Mylroie JE (2018) Diffuse versus conduit flow in coastal karst aquifers: The consequences of Island area and
676 perimeter relationships. *Geosci* 8:. <https://doi.org/10.3390/geosciences8070268>

677 Liu L, Shu L, Chen X, Oromo T (2010) The hydrologic function and behavior of the Houzhai underground river basin, Guizhou
678 Province, southwestern China. *Hydrogeol J* 18:509–518. <https://doi.org/10.1007/s10040-009-0518-z>

679 Maillet E (1905) *Essais d'hydraulique souterraine et fluviale*. Hermann

680 Mangin A (1975) *Contribution à l'étude hydrodynamique des aquifères karstiques*. Institut des Sciences de la Terre de
681 l'Université de Dijon

682 Marsaud B (1997) *Structure et fonctionnement de la zone noyée des karsts a partir des resultats experimentaux*

683 Mazzilli N, Guinot V, Jourde H, et al (2019) KarstMod: A modelling platform for rainfall - discharge analysis and modelling
684 dedicated to karst systems. *Environ Model Softw* 122:103927. <https://doi.org/10.1016/j.envsoft.2017.03.015>

685 Mudarra M, Andreo B (2011) Relative importance of the saturated and the unsaturated zones in the hydrogeological
686 functioning of karst aquifers: The case of Alta Cadena (Southern Spain). *J Hydrol* 397:263–280.
687 <https://doi.org/10.1016/j.jhydrol.2010.12.005>

688 Olarinoye T, Gleeson T, Marx V, et al (2020) Global karst springs hydrograph dataset for research and management of the
689 world's fastest-flowing groundwater. *Sci Data* 2020 71 7:1–9. <https://doi.org/10.1038/s41597-019-0346-5>

690 Padilla A, Pulido-Bosch A, Mangin A (1994a) Relative Importance of Baseflow and Quickflow from Hydrographs of Karst
691 Spring. *Ground Water* 32:267–277

692 Padilla A, Pulido-Bosch A, Mangin A (1994b) Relative Importance of Baseflow and Quickflow from Hydrographs of Karst
693 Spring. *Ground Water* 32:267–277. <https://doi.org/10.1111/j.1745-6584.1994.tb00641.x>

694 Perrin J, Jeannin PY, Zwahlen F (2003) Implications of the spatial variability of infiltration-water chemistry for the
695 investigation of a karst aquifer: A field study at Milandre test site, Swiss Jura. *Hydrogeol J* 11:673–686.
696 <https://doi.org/10.1007/s10040-003-0281-5>

697 Santos AC, Portela MM, Rinaldo A, Schaefli B (2019) Estimation of streamflow recession parameters: New insights from an
698 analytic streamflow distribution model. *Hydrol Process* 1–15. <https://doi.org/10.1002/hyp.13425>

699 Schuler P, Duran L, Johnston P, Gill L (2020) Quantifying and numerically representing recharge and flow components in a
700 karstified carbonate aquifer. *Water Resour Res*. <https://doi.org/10.1029/2020wr027717>

701 Sivelle V (2020) A methodology for the assessment of groundwater resource variability in karst catchments with sparse

702 temporal measurements

703 Stevanović Z (2018) Global distribution and use of water from karst aquifers. In: Geological Society Special Publication.

704 Geological Society of London, pp 217–236

705 Stoelzle M, Stahl K, Weiler M (2013) Are streamflow recession characteristics really characteristic? Hydrol Earth Syst Sci

706 17:817–828. <https://doi.org/10.5194/hess-17-817-2013>

707 Vogel RM, Kroll CN (1996) Estimation of Baseflow Recession Constants. Kluwer Academic Publishers

708 Vogel RM, Kroll CN (1992) Regional geohydrologic-geomorphic relationships for the estimation of low-flow statistics. Water

709 Resour Res 28:2451–2458. <https://doi.org/10.1029/92WR01007>

710 WMO (2008a) Manual on Low-flow Estimation and Prediction : Operational Hydrology Report No.50

711 WMO (2008b) Guide to Meteorological Instruments and Methods of Observation

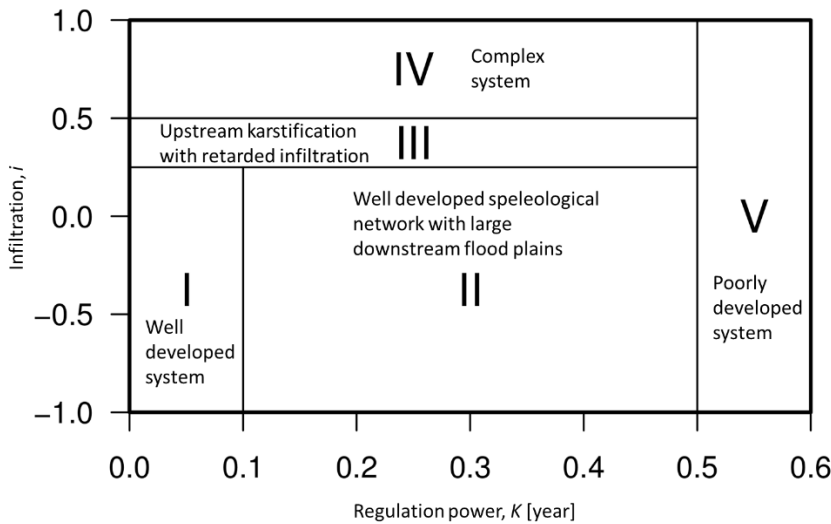
712 Xu B, Ye M, Dong S, et al (2018) A New Model for Simulating Spring Discharge Recession and Estimating Effective Porosity

713 of Karst Aquifers A new model for simulating spring discharge recession and estimating effective porosity of karst

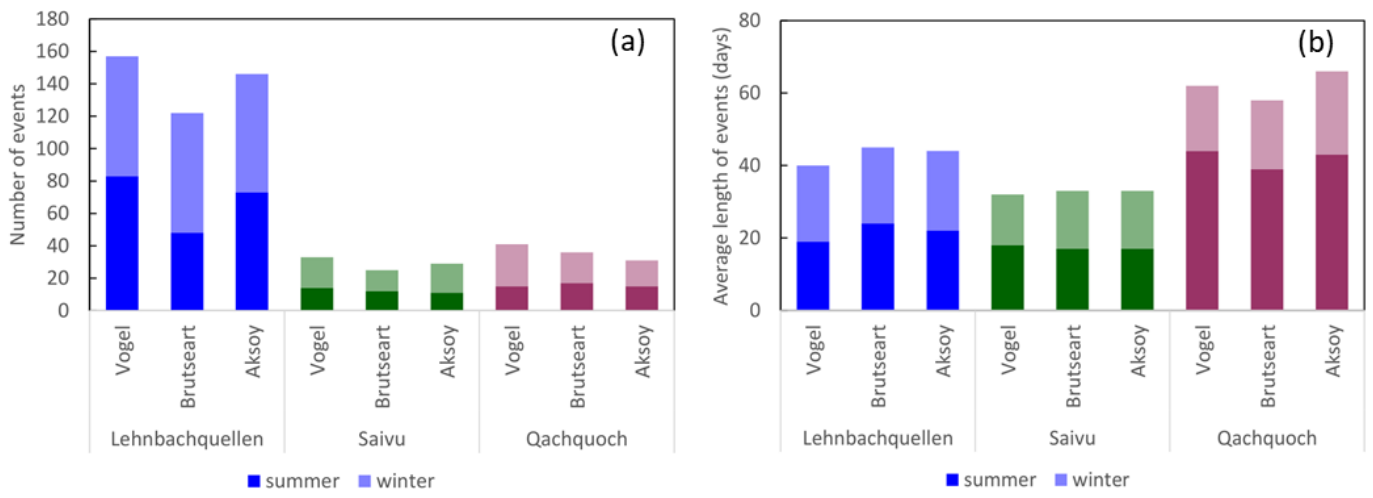
714 aquifers. J Hydrol 562:609–622. <https://doi.org/10.1016/j.jhydrol.2018.05.039>

715

716 **Appendix**



717
 718 Figure A1. The Mangin (1975) karst system classification scheme based on K and i .
 719
 720



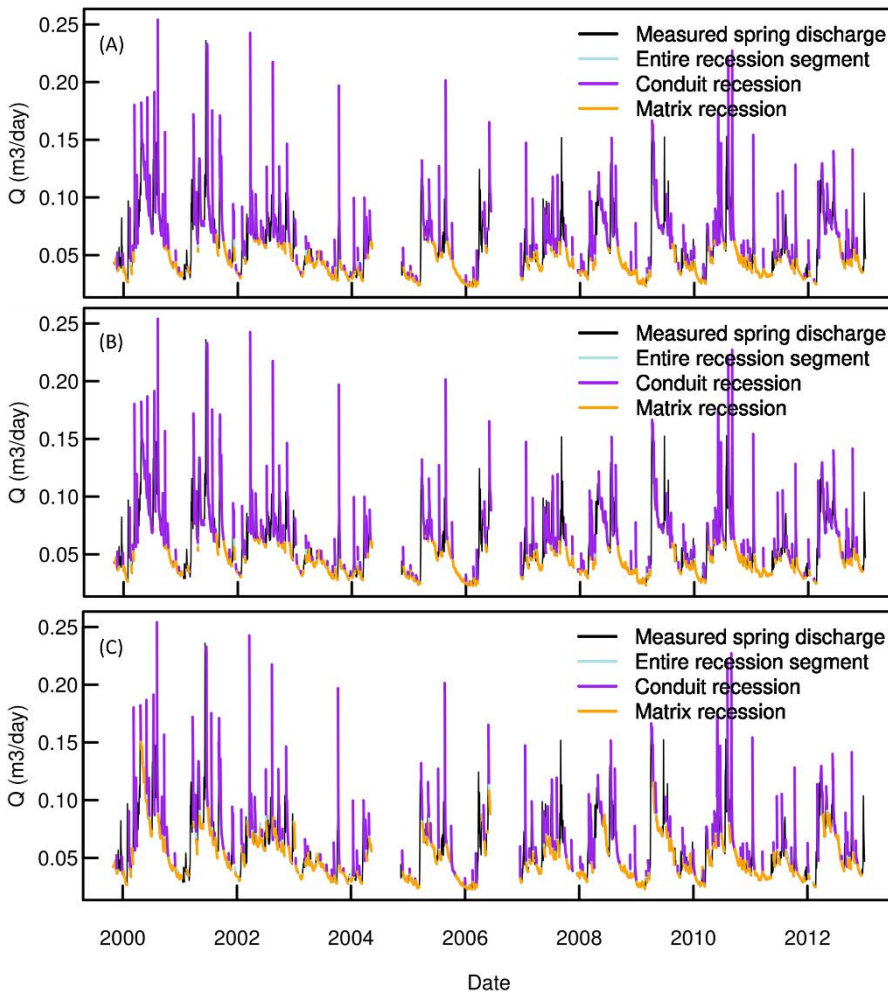
721

722

Figure A2. Characteristics of extracted recession events by REMs for both winter and summer periods in the three study sites: (a) number of identified complete recession events, and (b) the average number of days complete recession occurred.

723

724



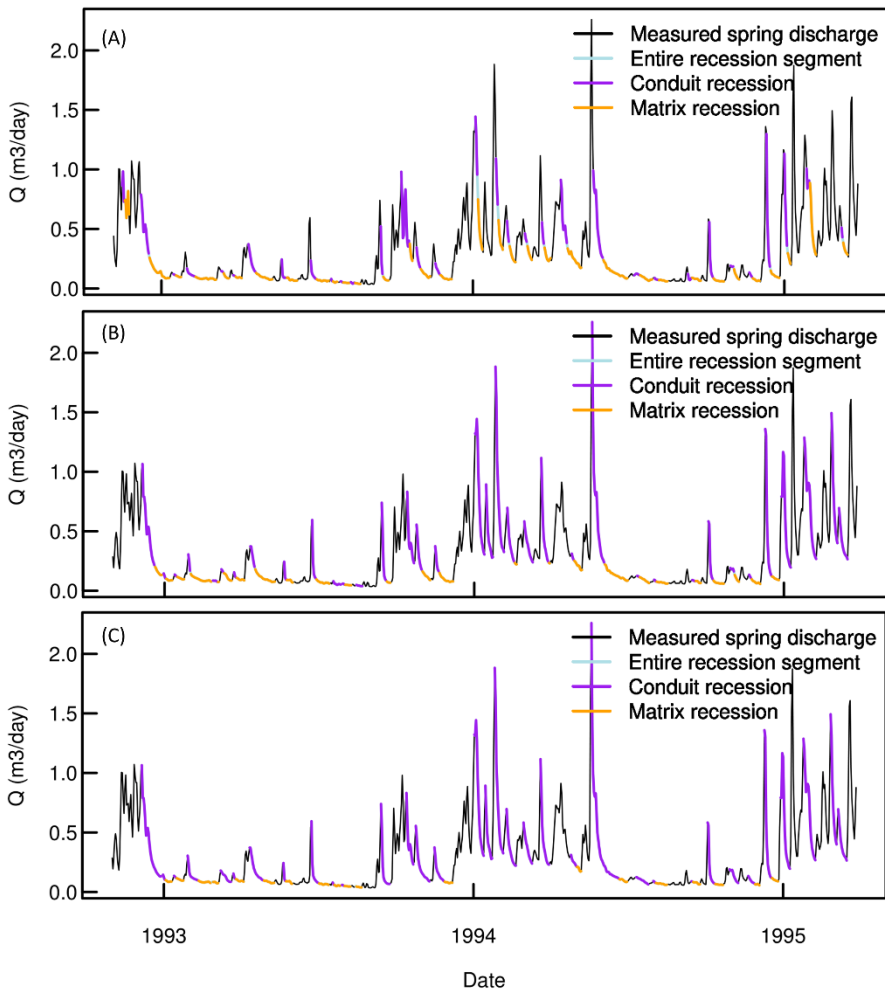
725

726

Figure A3. Lehnbachquellen spring discharge hydrograph and extracted recession events recognised by the three REMs: (A) Vogel, (B) Brutseart and (C) Aksoy.

727

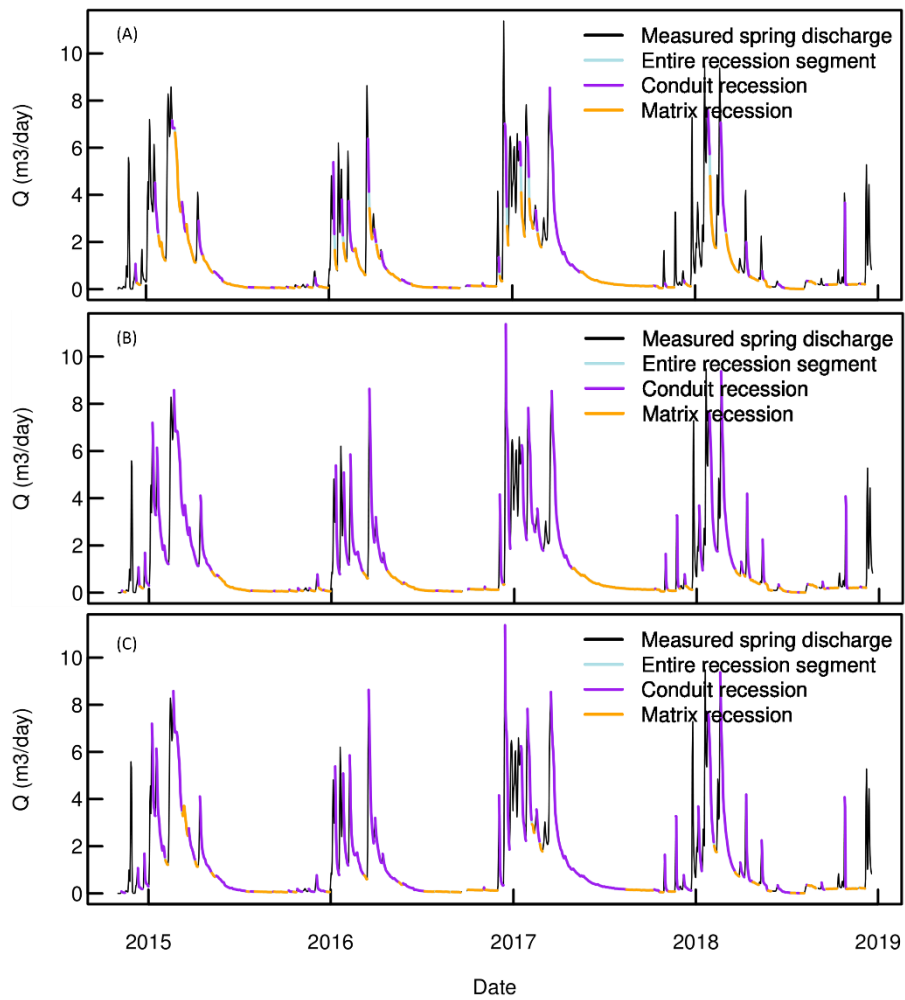
728



729

730 Figure A4. Saivu spring discharge hydrograph and extracted recession events recognised by the three REMs: (A) Vogel, (B) Brutseart and
 731 (C) Aksoy.

732



733

734 Figure A5. Qachquoch spring discharge hydrograph and extracted recession events recognised by the three REMs: (A) Vogel, (B) Brutseart
 735 and (C) Aksoy.

736